

## ESO Phase 3 Data Release Description

<b>Data Collection</b>	<VANDELS>
<b>Release Number</b>	<1>
<b>Data Provider</b>	<Ross McLure, Laura Pentericci>
<b>Date</b>	<11.09.2017>

### Abstract

This is the first data release (DR1) of the VANDELS survey, an ESO public spectroscopy survey targeting the high-redshift Universe. The VANDELS survey uses the VIMOS spectrograph on ESO's VLT to obtain ultra-deep, medium resolution, optical spectra of galaxies within the UKIDSS Ultra Deep Survey (UDS) and Chandra Deep Field South (CDFS) survey fields (0.2 sq. degree total area). Using robust photometric redshift pre-selection, VANDELS is targeting  $\approx 2100$  galaxies in the redshift interval  $1.0 < z < 7.0$ , with 85% of its targets selected to be at  $z \geq 3$ . In addition, VANDELS is targeting a substantial number of passive galaxies in the redshift interval  $1.0 < z < 2.5$ . Exploiting the red sensitivity of the refurbished VIMOS spectrograph, the survey is obtaining ultra-deep optical spectroscopy with the VIMOS MR grism and GG475 order-sorting filter, which covers the wavelength range 4800-10000Å at a dispersion of 2.5 Å/pix and a spectral resolution of  $R \sim 600$ . Each galaxy receives between a minimum of 20-hours and a maximum of 80-hours of on-source integration time. The fundamental aim of the survey is to provide the high signal-to-noise spectra necessary to measure key physical properties such as stellar population ages, metallicities and outflow velocities from detailed absorption-line studies. By targeting two extra-galactic survey fields with superb multi-wavelength imaging data, VANDELS is designed to produce a unique legacy dataset for exploring the physics underpinning high-redshift galaxy evolution.

A description of the survey and the primary science goals can be found in:

*"VANDELS: Exploring the Physics of High-redshift Galaxy Evolution"*  
 McLure R., Pentericci L. +VANDELS team  
 2017Msngr, 167, 31

### Overview of Observations

The VANDELS survey targets a total of eight VIMOS pointings, four pointings in the UDS field and four pointings in the CDFS field (see Fig. 1). Each VANDELS pointing has four associated masks, each of which is observed for 20-hours of on-source integration time. The survey utilizes a nested slit allocation policy, such that the brightest objects within a given pointing appear on a single mask (receiving 20-hours of integration), fainter objects appear on two masks (receiving 40-hours of integration) and the faintest objects appear on all four masks (receiving 80-hours of integration).

All observations were obtained using OBs designed to deliver a total of one-hour of on-source integration time. Each OB consisted of three integrations of 1200s, obtained in a three-point dither pattern, with dither off-sets of 0.82 arcseconds (dither positions 0,-0.82,1.64) corresponding to 4 pixels. One arc and one flat were obtained for calibration after the execution of two consecutive OBs. A spectrophotometric standard was observed at least once every 7 nights and at least once per run.

The nominal observing conditions required for a single exposure to be validated were: moon illumination below 0.5, seeing below 1.0 arcsecond FWHM, airmass below 1.5 and clear weather conditions. An exposure was still validated if one (and only one) of the above conditions was not met by less than 20% (e.g. seeing < 1.2") and all other conditions were satisfied. In Fig. 2 we show histograms of airmass, seeing and signal-to-noise ratio (S/N) for the spectra obtained during season one.

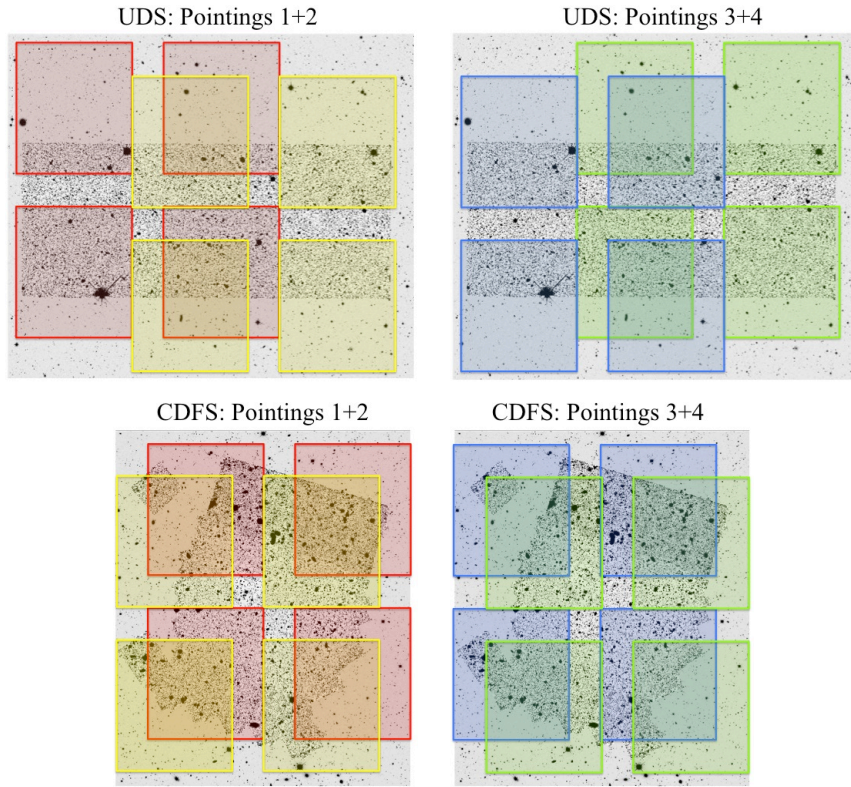


Fig 1. Layout of the eight VIMOS pointings within the UDS (top) and CDFS (bottom) fields. In each panel the background greyscale images show both the available *HST* (centre) and ground-based *HST* *H*-band imaging.

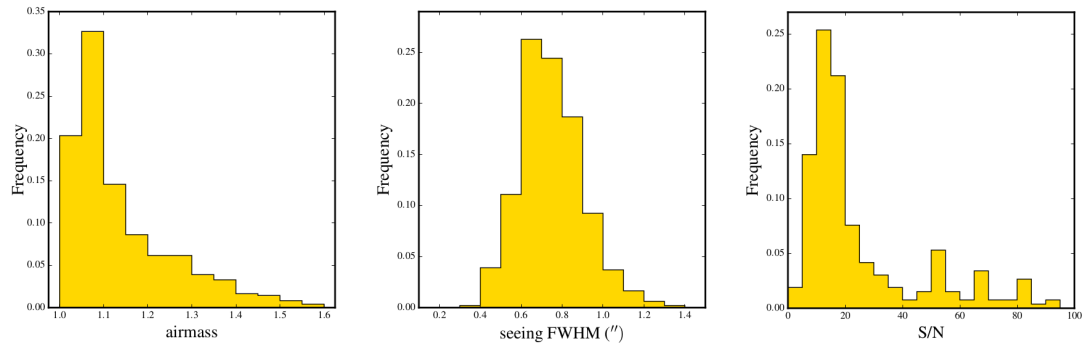


Fig 2. Histograms showing airmass, seeing and S/N ratios for the spectra obtained during season one. The first two panels show the airmass and seeing FWHM of the individual exposures, while the third panel shows the S/N ratio of the final spectra, measured per resolution element, in the wavelength range 6000-7000Å.

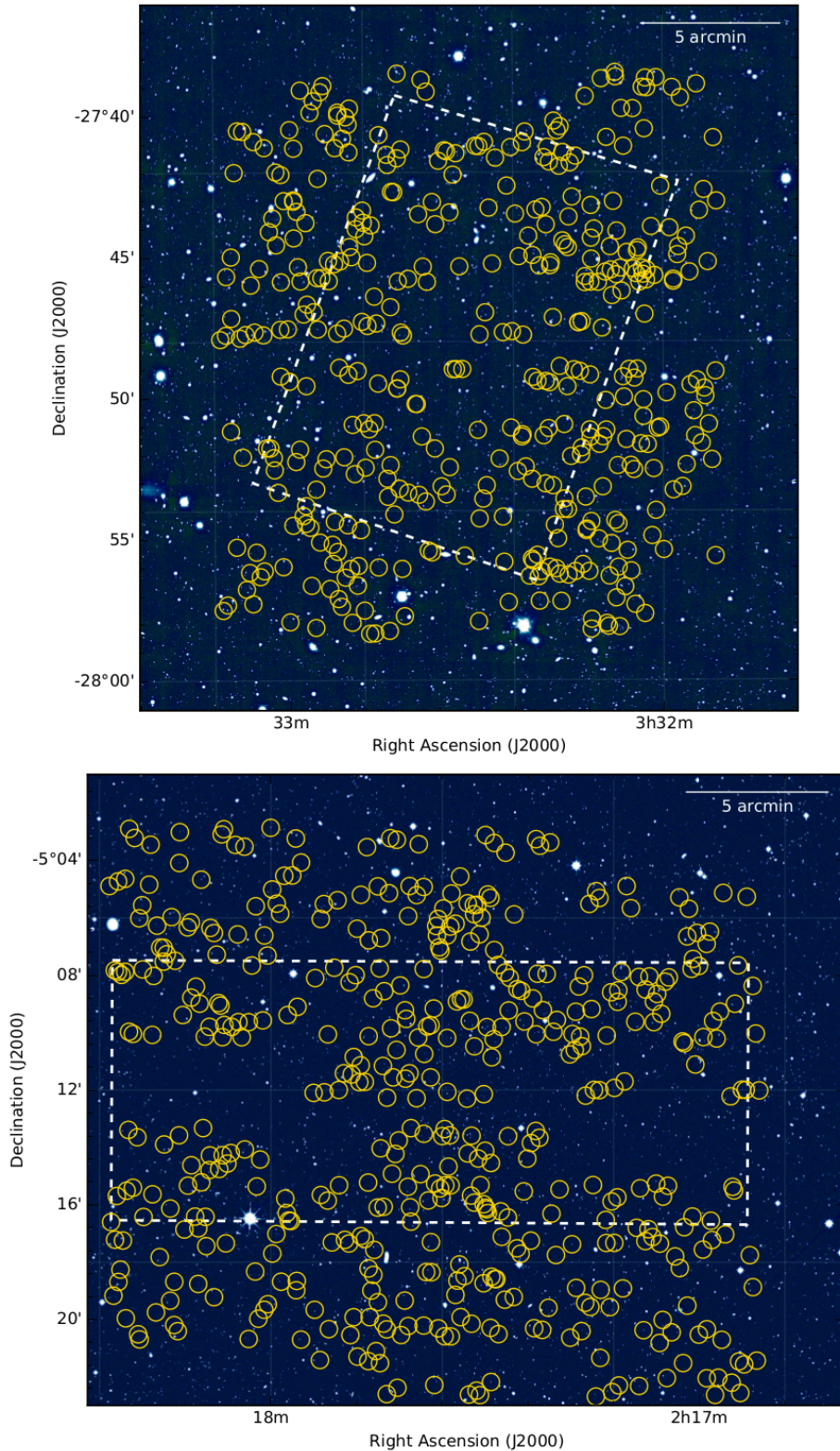


Fig. 3 Finding charts showing the location of the VANDELS DR1 spectra (yellow circles) within the CDFS (top) and UDS (bottom) fields. There are 415 spectra in the CDFS and 464 spectra in the UDS. The white dashed rectangles show the approximate location of the CANDELS near-IR Hubble Space Telescope imaging (Grogin et al. 2011). The background images are ground-based  $H$ -band data from the VISTA VIDEO survey (Jarvis et al. 2013) and UKIDSS UDS survey (Almaini et al., in prep) in the top and bottom panels respectively.

## Object Classification

All of the VANDELS targets were selected based on their photometric redshift and their  $i$ ,  $z$  &  $H$ -band magnitudes (full details will be provided in McLure et al., in prep). There are six target classifications in total (listed below), but the vast majority of the VANDELS spectra fall into the first three classes.

CLASS = PASS\_1.0\_z\_2.5 UVJ selected passive galaxies with  $1.0 < z_{\text{phot}} < 2.5$ ,  $H_{\text{AB}} < 22.5$ ,  $i_{\text{AB}} < 25$

CLASS = SF\_2.4<z<5.5 Bright star-forming galaxies with  $2.4 < z_{\text{phot}} < 5.5$ ,  $H_{\text{AB}} < 25$ ,  $i_{\text{AB}} < 25$

CLASS = LBG\_3.0<z<5.5 Fainter star-forming galaxies with  $3.0 < z_{\text{phot}} < 5.5$ ,  $H_{\text{AB}} < 27$ ,  $i_{\text{AB}} < 27.5$

CLASS = LBG\_5.5<z<7.0 Fainter star-forming galaxies with  $5.5 < z_{\text{phot}} < 7.0$ ,  $H_{\text{AB}} < 27$ ,  $z_{\text{AB}} < 27.5$

CLASS = AGN X-ray or radio-selected AGN candidates with  $z_{\text{phot}} > 2.4$ ,  $i_{\text{AB}} < 27.5$

CLASS = HERSCHEL Herschel detected galaxies with  $z_{\text{phot}} > 2.4$ ,  $i_{\text{AB}} < 27.5$

## Release Content

This data release consists of spectra obtained during the first VANDELS observing season, which ran from August 2015 until January 2016, ESO run numbers: 194.A-2003(E-K). The data release includes the spectra for all galaxies for which the scheduled integration time was completed during season one. In addition, the data release also includes the spectra for those galaxies for which the scheduled integration time was 50% complete at the end of season one (i.e. 20/40 hours and 40/80 hours).

The total number of spectra released is 879 (415 in CDFS and 464 in UDS) and the total data volume is 461 Mb.

The data release consists of

- Fully wavelength and flux calibrated 1D spectra for all 879 galaxies, along with the associated error spectrum and sky spectrum.
- Wavelength calibrated 2D spectra for all 879 galaxies.
- Catalogues listing the essential data associated with each galaxy (details below).

## Release Notes

### Data Reduction and Calibration

VANDELS data reduction was performed with a fully-automated pipeline, starting from the raw data and flowing down to the wavelength- and flux-calibrated spectra. The pipeline, called *Easy-life*, is an updated version of the algorithms and dataflow from the original VIPGI system, fully described in Scodreggio et al. (2005).

The first step in the reduction of VIMOS science data is the canonical preliminary reduction of the CCD frames, which includes prescan level and average bias frame subtraction, trimming of the frame to eliminate prescan and overscan areas, interpolation to remove bad CCD pixels and flat fielding. After the preliminary reduction step, subsequent data reduction steps are carried out on all MOS slits individually. For each individual spectroscopic exposure the wavelength calibration derived from the arc exposures is checked against the positions of bright sky lines and the local inverse dispersion solution modified to account for any discrepancies.

The next steps in the data reduction procedure are the object detection and sky subtraction for each MOS slit spectrum within each individual MOS science exposure. Initially, the slit spectrum is collapsed along the wavelength axis, following the geometrical shape defined by the local curvature model, to produce a slit cross-dispersion profile. A robust determination of the average signal level and r.m.s in this profile is then obtained using an iterative  $\sigma$ -clipping procedure, and objects are detected as groups of contiguous pixels above a given detection threshold. Before wavelength calibration is applied, a median estimate of the sky spectrum, derived using all the pixels that are devoid of object signal, is subtracted from each slit. The sky spectrum is estimated separately for each individual science exposure due to the significant variation in OH line strength over the timescale of a typical spectroscopic exposure.

The sky-subtracted slit spectra are then two-dimensionally extracted using the tracing provided by the slit curvature model, and resampled to a common linear wavelength scale. Only after this point are the single exposures of a pointing combined together. The  $N$  exposures that are part of a pointing are combined together twice. First, the  $N$  two-dimensionally extracted spectra for each slit are median combined (with object pixels masked), without taking into account the jitter offsets, to produce a two-dimensional sky-subtraction residual map.

The residual map is then subtracted from all the  $N$  two-dimensional single-exposure slit spectra, improving the sky-subtraction and removing any residual fringing. At this point a second combination is carried out, this time taking into account the jitter offsets among the  $N$  individual two-dimensional slit spectra (as determined during the previous object detection procedure). The single-exposure, residual-map subtracted, spectra are off-set to compensate for the effect of the jitter, and a final average two-dimensional spectrum for each slit is obtained.

The object detection process is repeated on the combined two-dimensional spectra to produce the final catalogue of detected spectra, and a one-dimensional spectrum is extracted for each detected object, using the Horne optimal extraction procedure (Horne 1986). Finally, spectra are flux calibrated using a simple polynomial fit to the instrument response curve derived from observations of spectrophotometric standard stars, and corrected for telluric absorption features. The last correction is based on a template absorption spectrum derived for each combined jitter sequence from the data themselves.

To perform the final flux calibration we adopt the procedure employed by the VIMOS Ultra Deep Survey (Le Fèvre et al., 2015), whereby the spectra are corrected for both atmospheric and galactic extinction before being normalized to the  $i$ -band photometry available for each target.

## Data Quality

The data quality control scheme implemented by VANDELS follows the successful system employed for the VIPERS survey (Garilli et al. 2012). This system carefully monitors the observing conditions for each scientific exposure. The seeing is directly measured from the raw spectroscopic data using bright reference objects. In addition, the median airmass of each exposure is computed on the basis of the observation hour angle and the airmass at the start and end of the observation. Moreover, the mean sky level is also measured and stored on an exposure basis. Finally, the accuracy of the individual slit wavelength calibrations computed via the inverse dispersion solutions is also monitored. All these data quality metrics are recorded in the FITS header of each individual spectrum.

Throughout the survey, all of these parameters are stored in a dedicated reduction database on an exposure by exposure basis. In the case of slit dependent values, such as wavelength calibration r.m.s. and sky level, the median value per quadrant per exposure is computed and recorded. Diagnostic plots showing the temporal behaviour of these parameters are made after each observing run. Observations showing some statistically significant deviation from the mean are flagged and their further use is subject of closer scrutiny, manually carried out by the reduction team.

## Spectroscopic Redshifts

Spectroscopic redshifts and associated quality flags have been determined for all objects in the current release using the Pandora software package, within the EZ environment (Garilli et al. 2010). The software simultaneously displays the 1D extracted spectrum, the 2D linearly resampled spectrum, the 1D sky spectrum and the noise. It is also possible to inspect the image thumbnail of the object with the exact position of the slit, to check for the presence of other sources in the same slit. The core algorithm for redshift determination is template cross-correlation, compared with a separate estimate of an emission line redshift when applicable. A key element for the cross-correlation engine to deliver a robust measurement is the availability of reference templates that cover a wide range of galaxy and star types and a wide range of rest-frame wavelengths. To determine the VANDELS spectroscopic redshifts we adopted templates derived from previous VIMOS observations for the VVDS (Le Fèvre et al. 2013) and zCOSMOS surveys (Lilly et al. 2007), with and without Lyman- $\alpha$  emission. Where necessary, it was also possible to set the redshift manually, e.g. by locating a single emission line in the spectrum. In several cases, it was necessary to manually perform some cleaning of the spectra, i.e. removing obvious noise residuals at the location of strong sky lines, or the zero-order projection.

Each target was assigned to two measurers from the VANDELS team who independently determined the redshift and located the main spectral features (in emission or absorption). Each measurer also assigned a spectroscopic quality flag to the target: these quality flags have been allocated according to the original system devised for the VVDS and are related to the confidence of the spectral measurement. The reliability flag may take the following values:

- 0: No redshift could be assigned (set to Nan)
- 1: 50% probability to be correct
- 2: 75% probability to be correct
- 3: 95% probability to be correct
- 4: 100% probability to be correct
- 9: spectrum with a single emission line. The redshift given is the most probable given the observed continuum, it has a >80% probability to be correct.

The quality flags for AGN spectra are preceded by an additional 1 (e.g 12, 14 etc), the quality flags for spectra which were not primary targets are preceded by an additional 2 and the quality flags for spectra deemed to be problematic are preceded by an additional -1.

Following their independent redshift determinations, the two measurers were required to compare their redshifts and flags and to reconcile any differences. As a final step, all spectra were also independently re-checked by the two PIs and any discrepancies in the redshifts and quality flags were again reconciled. This final pass was especially necessary to homogenize the quality flags as much as possible. Based on repeated measurements, the typical accuracy of the spectroscopic redshift measurements is estimated to be +/- 0.0005.

## Known issues

During final testing of the flux calibration of the DR1 spectra, it became clear that the extreme blue end of the spectra (i.e.  $\lambda < 5600\text{\AA}$ ) suffer from a systematic drop in flux when compared to the available photometry. The underlying cause for this loss of blue flux is still under investigation. For the purposes of this data release we have implemented an empirically derived correction to the spectra at  $\lambda < 5600\text{\AA}$ , which corrects for the flux loss on average.

The empirical correction, which has been applied to all of the DR1 spectra, is designed to ensure that the final spectra of bright star-forming galaxies in the redshift interval  $2.4 < z < 3.0$  display the expected power-law continuum slopes in the rest-frame wavelength range ( $1300\text{\AA} < \lambda < 2400\text{\AA}$ ), which are independently confirmed from the available photometry.

At the time of the data release, we believe that the spectra including the correction for blue flux loss represent our best calibration of the VANDELS spectra. However, given that we have applied an average empirical correction to the spectra at a relatively late stage before the data release, for completeness, we are also making available the spectra without the blue flux correction as an additional column of the 1D spectra fits table.

## Previous Releases

N/A

## References

Garilli et al., 2012, PASP, 124, 1232  
Garilli et al., 2010, PASP, 122, 827  
Grogin et al., 2011, ApJS, 197, 35  
Horne, 1986, PASP, 98, 609  
Jarvis et al., 2013, MNRAS, 428, 1281  
Le Fèvre et al., 2013, A&A, 559, 14  
Le Fèvre et al., 2015, A&A, 576, 79  
Lilly et al., 2007, ApJS, 172, 70  
McLure, Pentericci, et al., 2017, Msngr, 167, 31  
Scodreggio et al., 2005, PASP, 117, 1284

## Data Format

### Files Types

For each target the following data files are being released:

- the one-dimensional spectrum in FITS format, containing the following arrays
  - WAVE: wavelength in Angstroms (in air)
  - FLUX: 1D spectrum flux in  $\text{erg cm}^{-2} \text{s}^{-1} \text{angstrom}^{-1}$
  - ERR: noise estimate in  $\text{erg cm}^{-2} \text{s}^{-1} \text{angstrom}^{-1}$
  - UNCORR\_FLUX: 1D spectrum flux uncorrected for blue flux loss (see Known issues)
  - SKY: the subtracted sky in counts
- the two-dimensional resampled and sky subtracted (but not flux calibrated and atmospheric extinction corrected) spectrum in FITS format.

### Catalogue Columns

In addition to the one and two-dimensional spectra, we are releasing an associated catalogue divided into two tiles (*VANDELS\_UDS\_SPECTRO.fits* and *VANDELS\_CDFS\_SPECTRO.fits*), with the following columns:

NAME	DESCRIPTION	DATA TYPE	UNIT
id	The object ID	CHAR	
alpha	Right Ascension (J2000)	DOUBLE	deg
delta	Declination (J2000)	DOUBLE	deg
i_AB	The i-band magnitude	FLOAT	mag
i_FILTER	The i-band filter	STRING	
z_AB	The z-band magnitude	FLOAT	mag
z_FILTER	The z-band filter	STRING	
H_AB	The H-band magnitude	FLOAT	mag
H_FILTER	The H-band filter	STRING	
t_schedtime	The total requested integration time	INT	s
t_exptime	The current integration time	FLOAT	s
zphot	Photometric redshift	FLOAT	
zspec	Spectroscopic redshift	FLOAT	
zflg	Redshift measurement quality flag	FLOAT	
FILENAME	Fits filename of the ID spectrum	STRING	

Due to the heterogeneous nature of the ground-based and space-based imaging covering the UDS and CDFS survey fields, the *i*\_AB, *z*\_AB and *H*\_AB magnitudes listed in the release catalogues are generated from a number of different filters. The fundamental reason for this is the different photometry available for those targets selected within the areas covered by HST imaging (UDS\_HST and CDFS\_HST, ID numbers < 50,000) and those targets selected within the wider areas, primarily covered by ground-based imaging (UDS\_GROUND and CDFS\_GROUND, ID numbers > 100,000). Below we provide a guide to matching the catalogue photometry with the original filters:

- *i*\_AB magnitudes refer to the SUBARU *i*'-filter for the UDS\_GROUND and UDS\_HST targets, the F775W filter for CDFS\_HST targets and the SUBARU IA738 filter for the CDFS\_GROUND targets.
- *z*\_AB magnitudes refer to the SUBARU *z*'-filter for the UDS\_GROUND and UDS\_HST targets and the F850LP filter for the CDFS\_GROUND and CDFS\_HST targets.
- *H*\_AB magnitudes refer to the F160W filter for the UDS\_HST and CDFS\_HST targets, the WFCAM H-filter for the UDS\_GROUND targets and the VISTA H-filter for the CDFS\_GROUND targets.

For each object, the origin of the *i*\_AB, *z*\_AB and *H*\_AB photometry is listed in the catalogue in the *i*\_FILTER, *z*\_FILTER and *H*\_FILTER columns.

Due to changing observing conditions, some masks in both the UDS and CDFS fields have received more than their nominally scheduled 20 hours of on-source integration, resulting in objects in the catalogue with *t*\_exptime > *t*\_schedtime. In addition, to optimize slit allocation, six objects in this data release requiring 20 hours of on-source integration were placed on two VIMOS masks, and therefore actually received 40 hours of on-source integration.

## Acknowledgements

*VANDELS: Exploring the Physics of High-redshift Galaxy Evolution*

McLure R., Pentericci L. +VANDELS team

2017Msngr, 167, 31

Please use the following statement in your articles when using these data:

Based on data products from observations made with ESO Telescopes at the La Silla Paranal Observatory under programme ID 194.A-2003(E-K)